13th World Conference on Earthquake Engineering
Vancouver, B.C., Canada
August 1-6, 2004
Paper No. 1371

RECIPE FOR PREDICTING STRONG GROUND MOTIONS FROM FUTURE LARGE EARTHQUAKES

Kojiro IRIKURA[1], Hiroe MIYAKE[2], Tomotaka IWATA[3], Katsuhiro KAMAE[4], Hidenori KAWABE[5], and Luis Angel DALGUER[6]

SUMMARY

From recent development of the waveform inversion analyses for estimating rupture process using strong motion data during large earthquakes, we have understood that strong ground motion is relevant to slip heterogeneity inside the source rather than average slip in the entire rupture area. Asperities are characterized as regions that have large slip relative to the average slip on the rupture area, based on slip distributions estimated from the source inversion (Somerville *et al*. [1]). Then, the asperity areas as well as total rupture areas scale with seismic moment. We examined that strong motion generation areas approximately coincide with the asperity areas where stresses are largely released (Miyake *et al*. [2]). Based on the scaling relationships, the source model for the prediction of strong ground motions is characterized by three kinds of parameters, outer, inner, and extra fault parameters. The outer fault parameters are defined as entire rupture area and total seismic moment. The inner fault parameters are defined as slip heterogeneity inside the source, area of asperities, and stress drop on each asperity. We developed a recipe for predicting strong ground motions, which is to characterize the source model for the future large earthquakes. For the outer fault parameters, at first the total fault length is given as a sum of active fault segments. The fault width is related to thickness of seismogenic zones. The entire source area is defined as a product of the length and width, then the total seismic moment following the empirical scaling relationship. For the inner parameters, the area of asperities is estimated from the scaling with the total seismic moment. Stress drop on each asperity is derived based on a multiple-asperity model, which is given as an extension of a single-asperity model by Das and Kostrov [3]. The pattern of rupture nucleation and termination as the extra fault parameters are related to geomorphology of active faults and plates. We have examined the validity of the earthquake sources constructed by the recipe, comparing simulated and observed ground motions for recent large earthquakes, such as the 1995 Kobe and the 2003 Tokachi-oki earthquakes.

[1] Disas. Prev. Res. Inst., Kyoto University, Japan. Email: irikura@egmdpri01.dpri.kyoto-u.ac.jp
[2] Earthq. Res. Inst., University of Tokyo, Japan. Email: hiroe@eri.u-tokyo.ac.jp
[3] Disas. Prev. Res. Inst., Kyoto University, Japan. Email: iwata@egmdpri01.dpri.kyoto-u.ac.jp
[4] Res. Reac. Inst., Kyoto University, Japan. Email: kamae@kuca.rri.kyoto-u.ac.jp
[5] Res. Reac. Inst., Kyoto University, Japan. Email: kawabe@rri.kyoto-u.ac.jp
[6] Disas. Prev. Res. Inst., Kyoto University, Japan. Email: dalguer@egmdpri01.dpri.kyoto-u.ac.jp

INTRODUCTION

High-quality ground motions have been recorded from recent large earthquakes, such as the 1994 Northridge, the 1995 Kobe (Japan), the 1999 Kocaeli (Turkey), the 1999 Chi-Chi (Taiwan), and the 2003 Tokachi-oki (Japan) earthquakes. Accumulated data of strong ground motions have been providing us very important knowledge about rupture processes of earthquakes, propagation-path, and site-amplification effects on ground motion, the relation between ground motion and damage, and so on. Then, we have learned that earthquake damage resulted from destructive ground motion generated by rupture propagation effects inside the source as well as geological conditions. It shows that strong ground motion prediction is one of key factors for mitigating disasters for future earthquakes.

We made a framework of strong motion prediction as shown in Fig. 1. The strong motion from the scenario earthquake is evaluated from source modeling and Green's function estimation based on geological and geomorphological surveys of active faults, analyses of strong motion recordings, geophysical profiling of underground structures, and so on. The results will lead to improvement of the building code and bridge earthquake-resistant design.

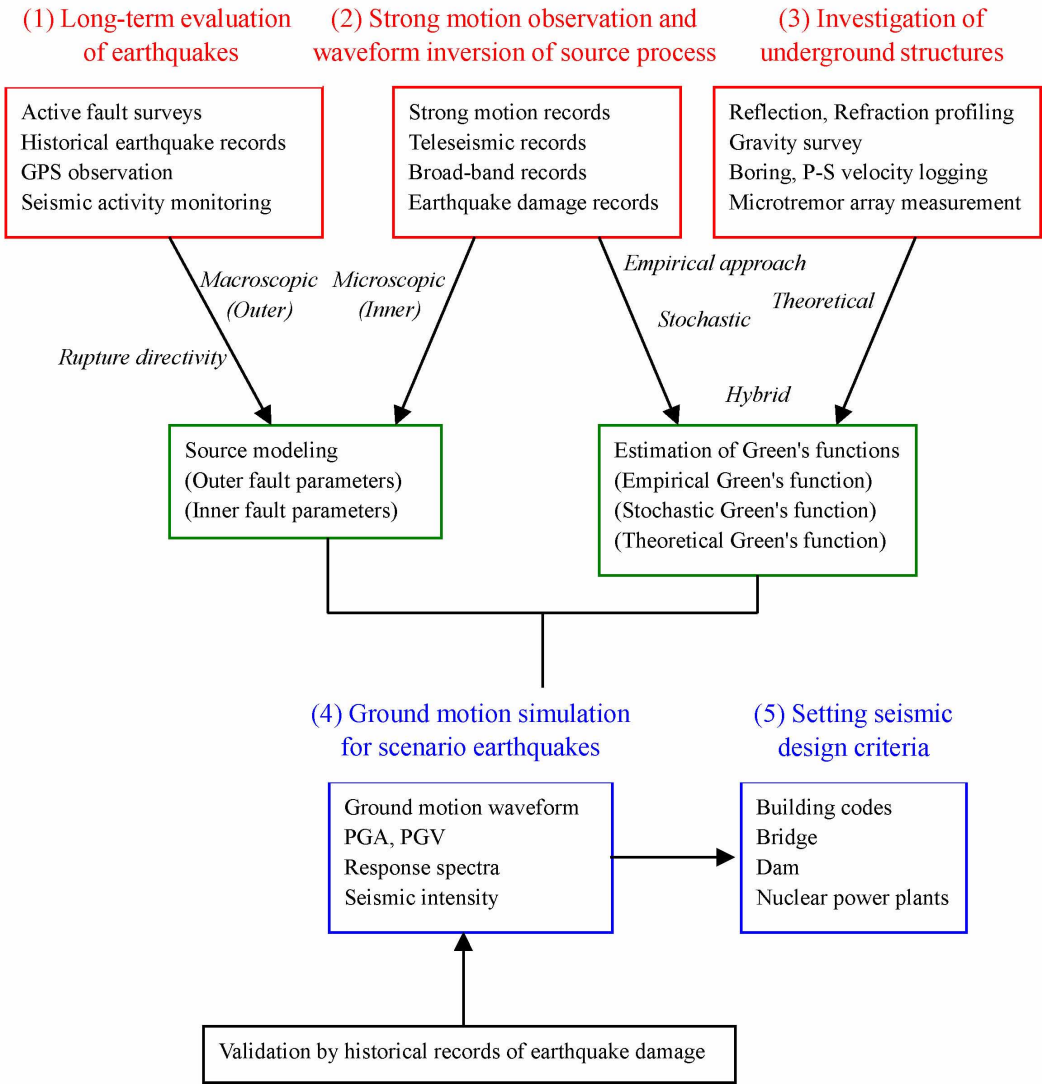

Fig. 1. Framework of predicting strong ground motion from scenario earthquake.

We attempted to make a recipe to popularize the prediction of ground motions for engineering purpose based on seismological fruits. There are two important factors for predicting strong ground motion, one is source characterization based on geological features for active faults and statistical analysis of source processes from the waveform inversion of strong motion records, the other is the estimation of the Green's functions from source to site.

For the former, we know that most of the uncertainties in predicting strong ground motion is to specify the proper methods of characterizing the source models of future earthquakes. We studied the scaling of the fault parameters based on the waveform inversion results of source process using the strong motion data. We found that the source model for estimating strong ground motion is characterized by three kinds of parameters, which we will call: outer fault parameter, inner fault parameters, and extra parameters, as discussed later.

For the latter, numerical Green's functions are calculated for ground motions longer than 1 sec based on methods such as Discrete Wave Number Method, Finite Deference Method, and Finite Element Method. The short period motions are estimated by the empirical Green's functions and stochastic simulation method for small events. To combine both methods, we introduce the idea of a hybrid scheme estimating broad-band Green's functions, deterministic and stochastic approaches in low (< 1 Hz) and high (> 1 Hz) frequency ranges, respectively, to obtain broad-band ground motions (Irikura and Kamae, [4]). Influence of variances of estimated source parameters on ground motions are discussed from synthetic waveforms based on our recipe.

BASIC IDEA FOR PREDICTING STRONG GROUND MOTION

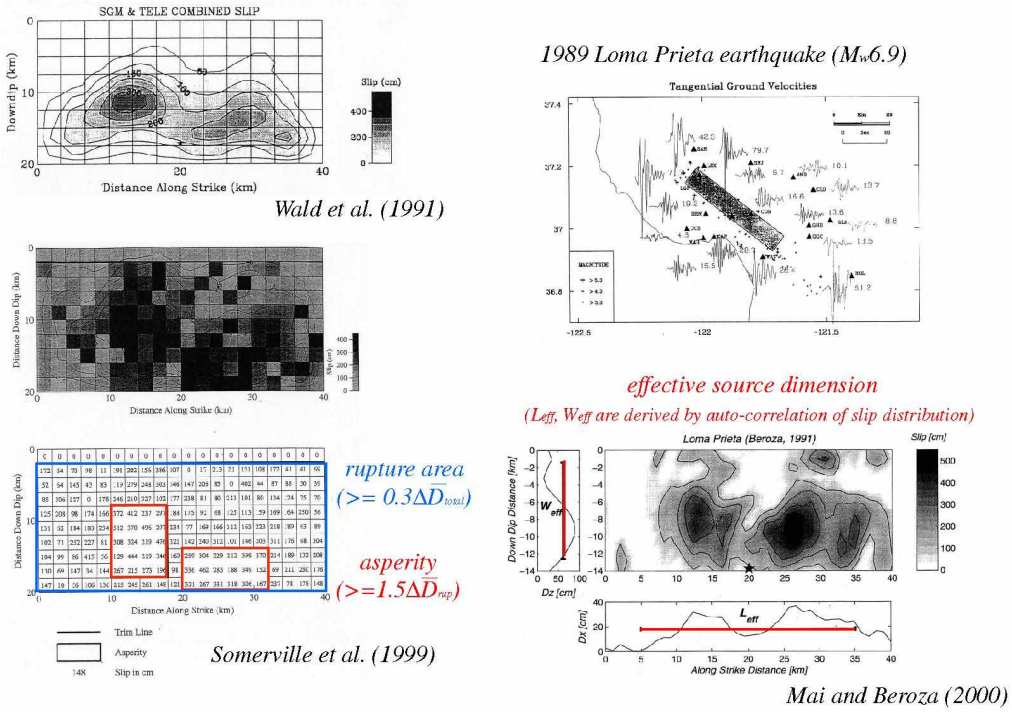

Fig. 2. Concept of source characterization based on the slip distributions by the waveforms inversions.

From recent development of the waveform inversion analyses for estimating rupture processes during large earthquakes, we have understood that strong ground motion is relevant to slip heterogeneity inside the source rather than the entire rupture area. The waveform inversion has shown that fault motions

consist of some asperities with large slip and background region with less slip (Fig 2). We have examined that strong motion generation areas approximately coincide with the asperity areas where stresses are released (Miyake *et al*. [2]). Such slip heterogeneity on the fault plane plays an important role on short period motions. Somerville *et al*. [1] found that slip heterogeneity inside the fault plane as well as entire rupture area follow the self-similar scaling laws with respect to total seismic moment. It suggests that source parameters for predicting ground motion are predictable when the total seismic moment or the source area for a future earthquake is given.

We introduce the idea of source characterization for predicting strong ground motion based on the multiple-asperity source model, which is given as an extension of a single-asperity source model by Das and Kostrov [3]. Relationship between the asperity-source model and source characterization is summarized in Fig. 3. Once distribution of the stress filed is characterized, dynamic simulation provides slip distribution. The procedure of the source characterization is derived high stress region from the slip distribution obtained by the waveform inversions.

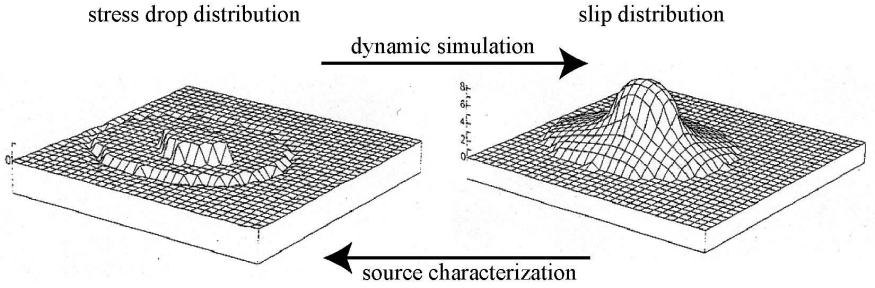

Fig. 3. Asperity source model for simulating strong ground motions. Distribution of stress change (left) and final slip (right) for a single-asperity source model (after Boatwright [7]).

For a single-asperity source model, where an asperity locates in arbitrary position inside the stress-free field, seismic moment, stress drop on the asperity, and acceleration source-spectral level are derived as follows.

$$M_0 = \frac{16}{7}\Delta\sigma_a r^2 R \qquad (1)$$ from Boatwright [7] based on Das and Kostrov [3]

$$\Delta\sigma_a = \frac{7}{16}\frac{M_0}{Rr^2} \qquad (2)$$ from Boatwright [7] based on Das and Kostrov [3]

$$A_0^a = 4\pi\beta v_r \Delta\sigma_a r \qquad (3)$$ from Madariaga [8]

where β is *S*-wave velocity and v_r is rupture velocity. These equations are extendable for the multiple-asperity source models, taking into account that low frequency motions from plural asperities are coherently summed while high frequency motions are randomly summed. The low and high frequency motions are related to the seismic moment and the acceleration level, respectively. Regardless of the number of asperities, the stress drop on each asperity is the same as long as the sum of the asperity areas is constant. Stress drop on the asperities $\Delta\sigma_a$ is derived as a multiple of the average stress drop over the fault $\Delta\overline{\sigma}_c$ and the ratio of asperity area S_a to total rupture area S (e.g., Madariaga, [9]).

$$\Delta\sigma_a = \Delta\overline{\sigma}_c \cdot \frac{S}{S_a} \qquad (4)$$

FUNDAMENTAL RELATIONSHIPS CONTROLLING FAULT PARAMETERS

Scaling Relations of Outer Fault Parameters

The outer fault parameters are parameters characterizing the entire source area such as total rupture area and seismic moment. Conventional scaling relations of the fault parameters such as fault length and average slip on fault with seismic magnitude are mostly determined geologically from surface offsets and geophysically from forward source modeling using teleseismic data and geodetic data. Those data are only available for very long period motions but not enough for near-source strong motions dominating short period motions less than 1 sec of engineering interest.

We examined the scaling relations of seismic moment versus total rupture area based on the statistical analysis of source processes from the waveform inversion of strong motion records from crustal earthquakes (Somerville *et al*. [1]; Miyakoshi [10]). Analyzed data range from M_w 5.7 to M_w 7.6. For moderate-size earthquakes, the total fault area S follows the self-similar scaling relation with seismic moment M_0 expressed as equation (5) by Somerville *et al*. [1]. For larger earthquakes, we proposed the scaling departing from self-similar model (Irikura and Miyake [11]) adding the reliable data from Wells and Coppersmith [12] to support the saturation of the fault width. This scaling shown in equations (5) and (6) has been also found in Hanks and Bakun [13]. For extra large earthquakes, we quoted the idea by Scholz [14] changing from *L*-model into *W*-model. Relationship between seismic moment and rupture area for inland crustal earthquakes are summarized. Saturation of the fault width is assumed as 20 km.

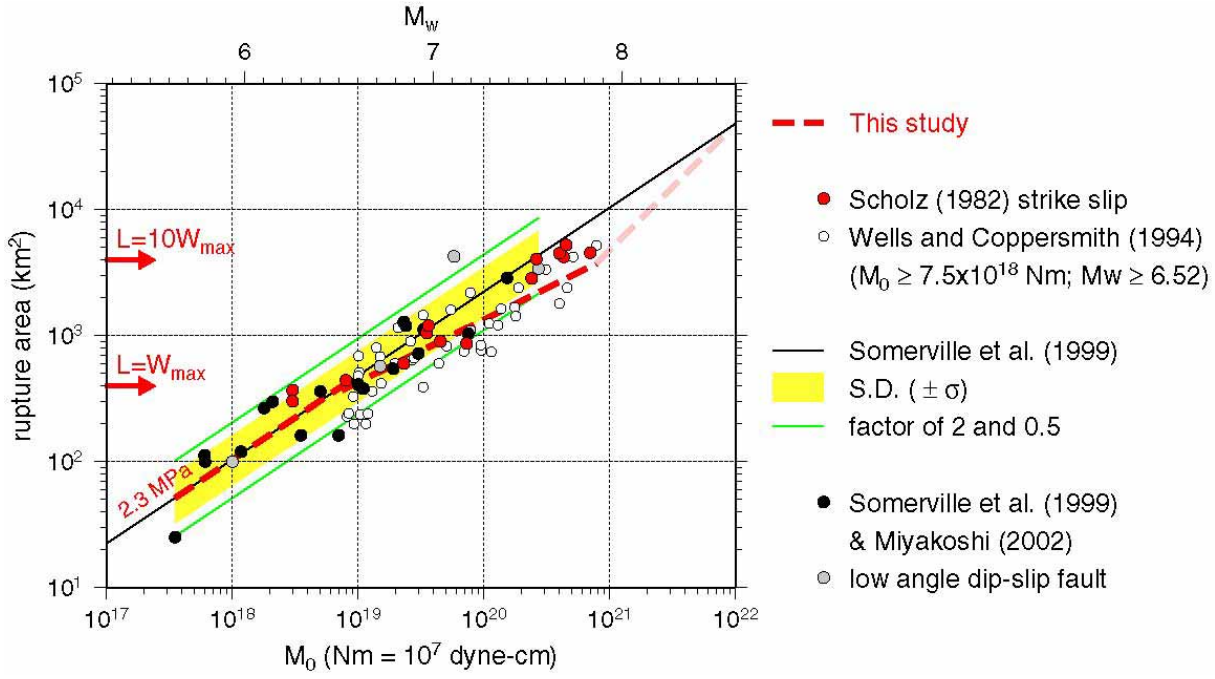

Fig. 4. Empirical relationship between seismic moment and rupture area for inland crustal earthquakes. Thick broken lines are 3-stage scaling relationships proposed by our studies (e.g., Irikura *et al*. [15])

$S\ (km^2) = 2.23 \times 10^{-15} \times Mo^{2/3}$	for $Mo < 7.5 \times 10^{25}$ dyne-cm	(5)	after Somerville *et al*. [1]
$S\ (km^2) = 4.59 \times 10^{-11} \times Mo^{1/2}$	for $Mo >= 7.5 \times 10^{25}$ dyne-cm	(6)	after Irikura and Miyake [11]
$S\ (km^2) = 5.30 \times 10^{-25} \times Mo$	for $Mo >= 7.5 \times 10^{27}$ dyne-cm	(7)	

To support our proposed scalings, we developed a series of dynamic rupture simulations rectangular sources with homogeneous stress drop with boundary condition of surface and sub-surface

earthquakes (Fig. 5). The relationship between the seismic moment and the total rupture area is shown in Fig. 6, and that between the fault length and average slip in Fig. 7.

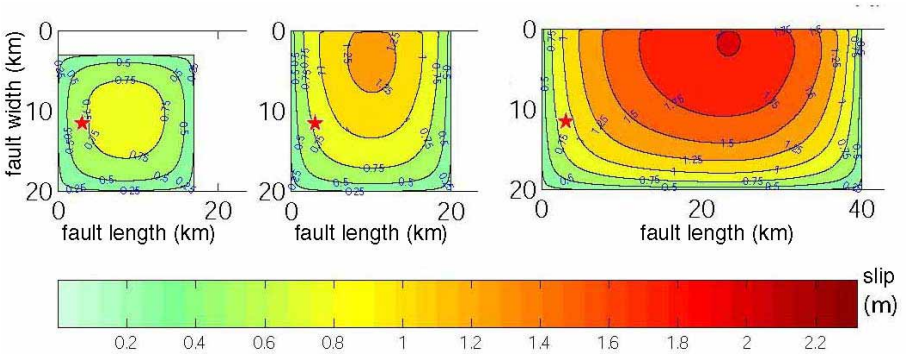

Fig. 5. Several examples of final slip distribution for rectangular crack models by dynamic simulations.

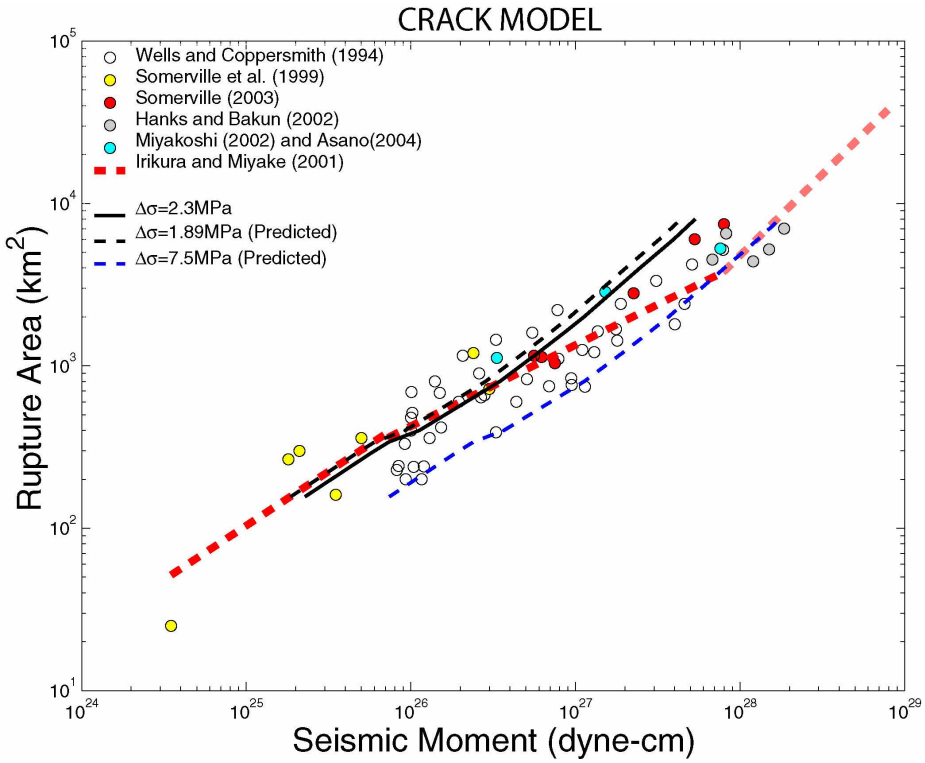

Fig. 6. Relationship between seismic moment and total rupture area for inland crustal earthquakes from dynamic simulations. W_{max} is assumed as 20 km.

We propose a 3-stage scaling relationship between seismic moment and rupture area for both inland crustal and subduction-zone earthquakes. The first stage is a scaling with constant static stress drop before fault width saturating the seismogenic zone, the second stage is a scaling increasing static stress drop after the saturation of fault width, then the third stage is a scaling with constant static stress drop again where the fault length becomes long enough. Source-scaling implied from dynamic rupture simulation explains the circular-crack model, *L*-model, and *W*-model together cooperating with the idea by Scholz [14].

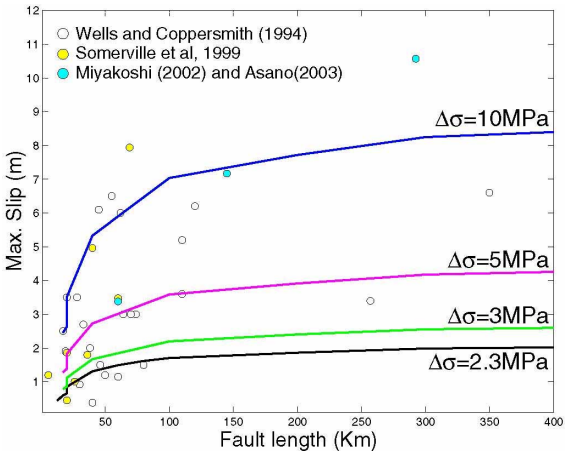

Fig. 7. Relationship between fault length and maximum slip from dynamic simulations.

Scaling Relations of Inner Fault Parameters

Strong ground motions are controlled by inner fault parameters for slip heterogeneity as well as outer fault parameters defining the entire rupture area and total seismic moment. Fig. 8 displays the relationship between rupture area S as the outer fault parameter and combined area of asperities S_a as the inner fault parameter, according to the waveform inversion results compiled by Somerville *et al*. [1] and Miyakoshi [10]. S_a / S seems to be constant regardless of the rupture area.

$$S_a / S = 0.215 \qquad (8)$$

after Irikura and Miyake [11]

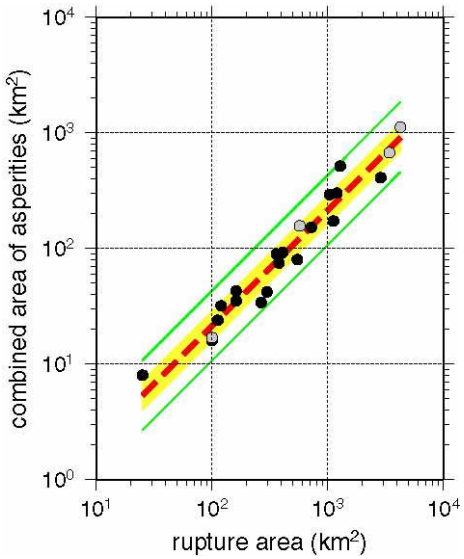

Fig. 8. Empirical relationship between combined area of asperities and total rupture area (thick broken line) for inland crustal earthquakes. Shadow ranges $\pm\sigma$ (standard deviation). Thin solid lines show a factor of 2 and 1/2 for the average (after Irikura and Miyake [11]). Database obtained by the waveform inversions for the inland crustal earthquakes is Somerville *et al*. (1999) and Miyakoshi (2002).

When the relationship between combined area of asperities and total rupture area is not given or unclear, there is a choice to practice the relationship between seismic moment and acceleration source spectral level. By using the relationships $A_0 \propto M_0^{1/3}$ obtained empirically (Fig. 9) and ${A_0}^a \propto M_0^{1/3}$ theoretically from equation (3) together, the combined of asperities are derived as follows.

$$S_a = \left(\frac{7\pi^2}{4} \beta v_R \right)^2 \cdot \frac{(M_0)^2}{S \cdot ({A_0}^a)^2} \qquad (9)$$

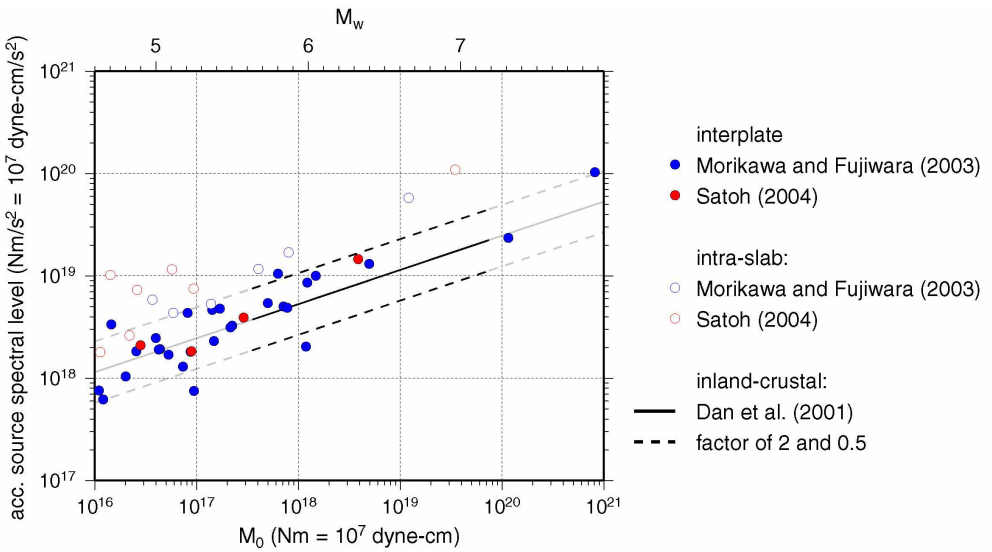

Fig. 9. Empirical relationship between seismic moment and acceleration source spectral level for the subduction-zone earthquakes.

Constraints on Average Slip of Asperities from Dynamic Simulations

Slip distribution for the multiple-asperity source models is dynamically solved by numerical simulation. The simulations suggest that even identical seismic moment decreases D_a/D with increasing of the number of asperities, where D_a and D are average slip of the asperities and the entire fault, respectively (Fig. 10).

(a)

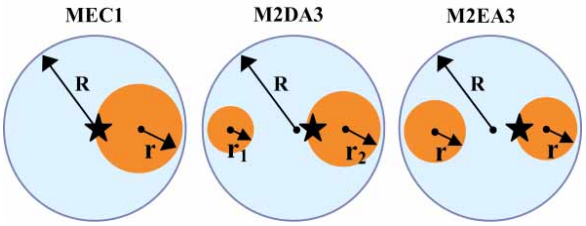

(b)

$\Delta\sigma_b/\Delta\sigma_a = 0.0$			
	MEC1	M2DA3	M2EA3
Masp/Mo	0.530	0.458	0.450
Dasp/D	2.363	2.052	2.027
Dmax/D	2.921	2.638	2.476

(c)

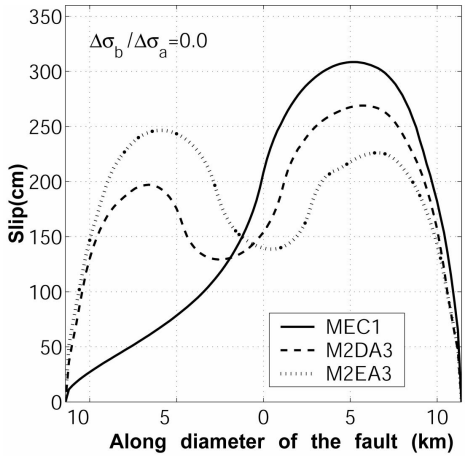

Fig. 10. Dynamic solution of three selected circular asperity models with fixed rupture velocity (0.8Vs) and critical slip D_c = 0.4 m. (a) Asperity location for each circular fault model. Star represents the rupture starting point, R and r are the radii of the fault and asperity. The ratio between the combined asperity area (S_a=90km^2) and total rupture area (S=408km^2) is 0.22. This ratio is partitioned for the double asperities, 11% for each asperity of model M2EA3 and 6%-16% for M2DA3. The stress drop in the asperity is $\Delta\sigma_a$=10.5 MPa. (b) The table specifies the ratios of seismic moment (M_{asp}/M_0), average slip (D_{asp}/D), and maximum slip (D_{max}/D) between the asperity area and total rupture area in case of $\Delta\sigma_b/\Delta\sigma_a = 0$. (c) Final slip distribution along the diameter of the fault (in-plane direction) in the case of $\Delta\sigma_b/\Delta\sigma_a = 0$.

RECIPE FOR CHARACTERIZING EARTHQUAKE SOURCE

We outline the procedure for characterizing the source model to estimate strong ground motion for future large earthquake. For estimating strong ground motions using a deductive approach, we need to have three kinds of source parameters, outer, inner, and extra fault parameters.

Outer Fault Parameters -Estimation of Seismic Moment for Possible Earthquake-

Step 1: Total Rupture Area ($S = LW$)

Total fault length L of the possible earthquake is defined as sum of the lengths of the fault segments grouping simultaneously activated. Fault width W is related to the total fault length before reaching the thickness of the seismogenic zone W_{max}.

W (km) = L (km) for $L < W_{max}$ (10)

W (km) = W_{max} (km) for $L >= W_{max}$ (11)

Step 2: Average Stress Drop ($\Delta\overline{\sigma}_c$) on the Fault

The average stress drop is assumed depending on the rupture size or depth dependency.

Step 3: Total Seismic Moment (M_0)

When crack-like fault model is adopted, Eshelby [22]'s equation is applied.

Otherwise, relationship between seismic moment and rupture area would be considered.

$$M_0 = \frac{16}{7\pi^{1.5}} \Delta\overline{\sigma}_c \cdot S^{1.5} \quad (12)$$

Inner Fault Parameters - Slip Heterogeneity or Roughness of Faulting -

Step 4. Combined Area of Asperities (S_a)

From the empirical relation of Sa-S (Somerville *et al*. [1]; Irikura and Miyake [11]), where the combined area of asperities is specified to be about 22%.

Step 5. Stress Drop on Asperities ($\Delta\sigma_a$)

As shown in equation (4), $\Delta\sigma_a$ as the inner fault parameter is derived as a multiple of $\Delta\overline{\sigma}_c$ as the outer fault parameter and S_a/S from Step 4.

Step 6. Number of Asperities (N)

The asperities in the entire fault rupture are related to the segmentation of the active faults or to information of past earthquakes. Locations of the asperities are from surface offsets measured along fault or from back-slip rate studied by GPS observation.

Step 7: Average Slip on Asperities (D_a)

Based on Step 6 and empirical relationships from dynamic simulations of the slip distribution for the multiple-asperity source model.

(Examples: $D_a/D = 2.3$ for $N = 1$, $D_a/D = 2.0$ for $N = 2$, $D_a/D = 1.8$ for $N = 3$)

Step 8: Effective Stress on Asperity (σ_a) and Background Slip Areas (σ_b)

We treat stress drop on asperity ($\Delta\sigma_a$) as effective stress (σ_a) on asperity for strong motion generation. The effective stress on background slip area is constrained by the empirical relationship between seismic moment and acceleration source spectral level.

Step 9: Parameterization of Slip-Velocity Time Functions

Modeling of peak slip-velocity and rise time for both asperity and background areas.

Extra Fault Parameters - Propagation Pattern of Rupture -

The extra fault parameters are related to the fault geometry rupture starting point, characterizing

rupture propagating pattern, and rupture velocity. For inland crustal earthquakes, rupture nucleation and termination are related to geomorphology of active faults (e.g., Nakata *et al*. [23]; Kame and Yamashita [24]). For subduction-zone earthquakes, information from past earthquakes is applied as possible.

EXAMPLES FOR SIMULATING STRONG GROUND MOTION

Inland Crustal Earthquake: 1995 Kobe Earthquake

We have successfully made characterize earthquake rupture models for the prediction of ground motions from statistical analysis of the source inversion results for inland crustal earthquakes. Cooperating with high-quality ground motion records from recent earthquakes in California, Japan, and Taiwan, we verified the applicability of the methodology comparing simulated ground motions with observed ones for the 1994 Northridge, 1995 Kobe, 1999 Kocaeli, and 1999 Chi-Chi earthquakes. Fig. 11 shows the ground motion simulation following the recipe, for the 1995 Kobe earthquake, Japan, by Irikura *et al*. [25] using the stochastic Green's function method.

(a)

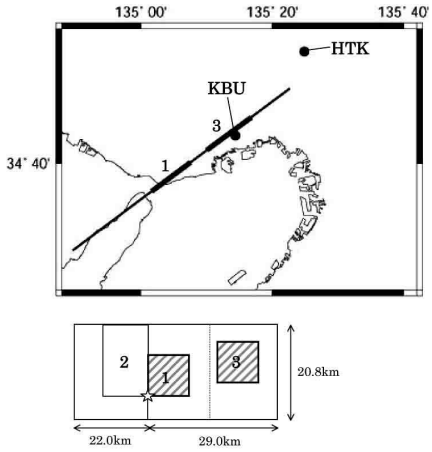

(b)

	M_0 dyne-cm	S km²	D cm	$\Delta\sigma$ MPa	A dyne-cm/sec²
total fault area	3.29×10^{26}	1062	103	2.3	1.70×10^{26}
segment 1 (total)	8.43×10^{25}	300	94	2.3	9.03×10^{25}
(asperity)	3.57×10^{25}	64	186	10.5	7.29×10^{25}
(background)	4.86×10^{25}	236	69	4.0	5.33×10^{25}
segment 2 (total)	1.60×10^{26}	462	115	2.3	1.12×10^{26}
(asperity)	6.96×10^{25}	100	232	10.5	9.12×10^{25}
(background)	9.04×10^{25}	362	83	4.0	6.50×10^{25}
segment 3 (total)	8.43×10^{25}	300	94	2.3	9.03×10^{25}
(asperity)	3.57×10^{25}	64	186	10.5	7.29×10^{25}
(background)	4.86×10^{25}	236	69	4.0	5.33×10^{25}

(c)

(d)

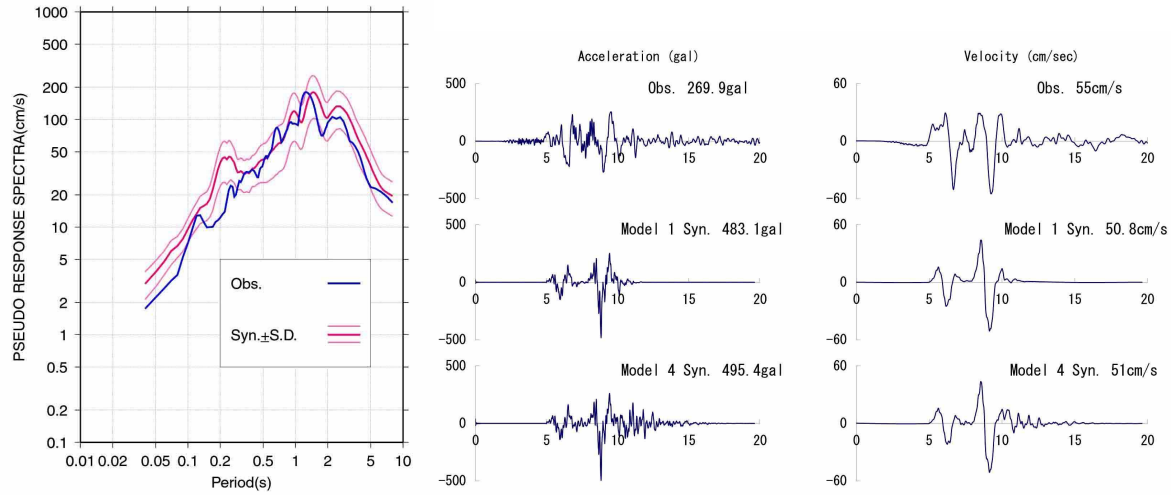

Fig. 11. Ground motion simulation for the 1995 Kobe earthquake using the stochastic Green's function method. (a) Characterized source model based on Kamae and Irikura [26]. (b) Source parameters. (c) Variability of simulated response spectra for 10 different element earthquakes. (d) Comparison between observed and simulated velocities of NS component at KBU station.

Subduction-Zone Earthquake: 2003 Tokachi-oki Earthquake

For subduction-zone earthquakes, accurate source inversion results have not been obtained enough to make scaling relations of source heterogeneities. Some inversion results using near-field displacements with low-amplification seismographs and teleseismic data from the 1944 Tonankai and 1946 Nankai earthquakes as well as those using the strong motion records from the 1985 Michoacan earthquake have showed slip-heterogeneity scaling similar to the inland earthquakes. We apply the procedure similar to the inland earthquakes to estimating strong ground motions from the subduction-zone earthquakes. Fig. 12 shows the source modeling for strong ground motion from the 2003 Tokachi-oki earthquake, Japan, by Kamae and Kawabe [27] using the empirical Green's function method.

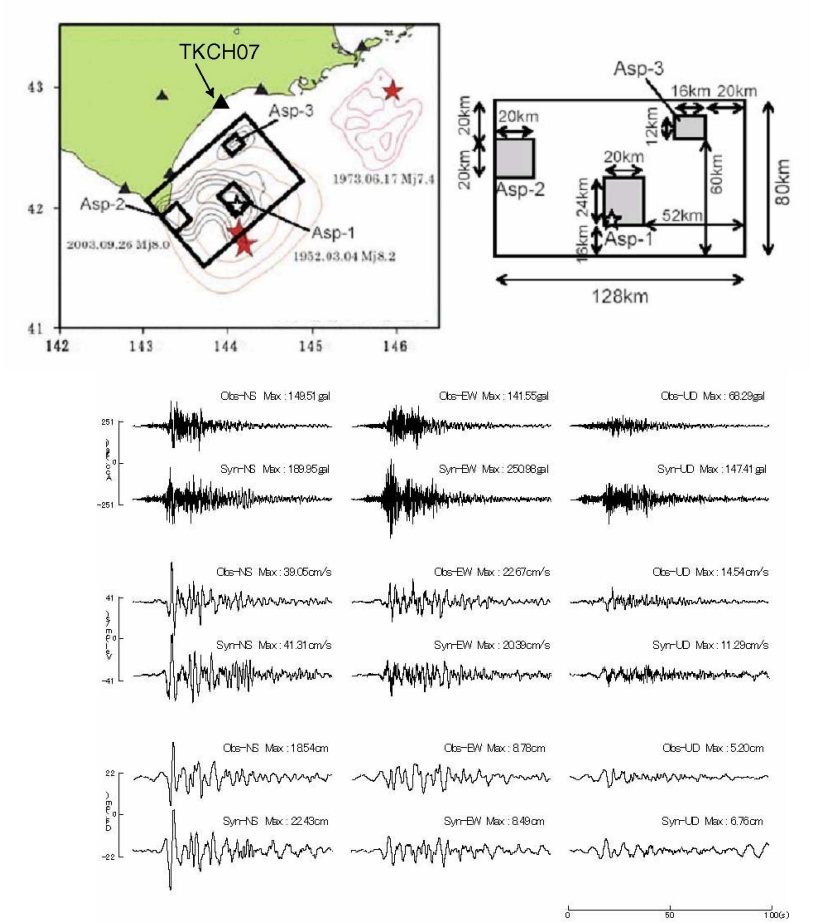

Fig. 12. Ground motion simulation for the 2003 Tokachi-oki earthquake (after Kamae and Kawabe [27]) using the empirical Green's function method. Upper: characterized source modeling consists of three asperities. Black contours show the slip distribution in every 1m obtained by Yamanaka and Kikuchi [28]. Lower: comparison between observed and simulated waveforms for TKCH07 station.

DISCUSSION

Are Asperities Repetitious?

Estimation of the asperity location from future earthquakes is challenging issue as well as central importance for the source characterization. As some proofs of the characteristic source models, Kikuchi and Yamanaka [29] has been proposed the repetition of asperities for subduction-zone earthquakes, comparing the source inversion results for both present and past large earthquakes by retrieving the historical waveforms. Fig. 13 displays that the location of asperities seems to be overlapped for the event pairs of the 1952 and the 2003 Tokachi-oki earthquakes by Yamanaka and Kikuchi [28], and for the 1968 Tokachi-oki and the 1994 Sanriku-Oki earthquakes by Nagai *et al*. [30].

How to Find the Asperities?

Geological, geomorphological, seismological, geodetic surveys imply the information to locate the asperities.

- Coincidence of surface offsets measured along active fault and locations of asperities on fault segments: Wald and Heaton [31] for the 1994 Landers earthquake and by Lee *et al*. [32] and Iwata *et al*. [33] for the 1999 Chi-Chi earthquake.
- Seismic activity: Less active inside asperities and relatively more active surrounding the asperities before the earthquake. Measuring b values, a values, and local recurrence time as indication where asperities may be located (Wyss *et al*. [34]).
- Reflected (scattered) waves: strong/less reflection (scattering) coefficients inside asperities and relatively high outside asperities. Locked segments with weaker scattering and low microseismicity, and segment boundaries with stronger scattering and stationary microseismicity. The locked segments are ruptured as asperities for future earthquakes (Nishigami [35]).
- Back-slip estimation from by GPS analyses indicating coupling-rate of the plate boundary.

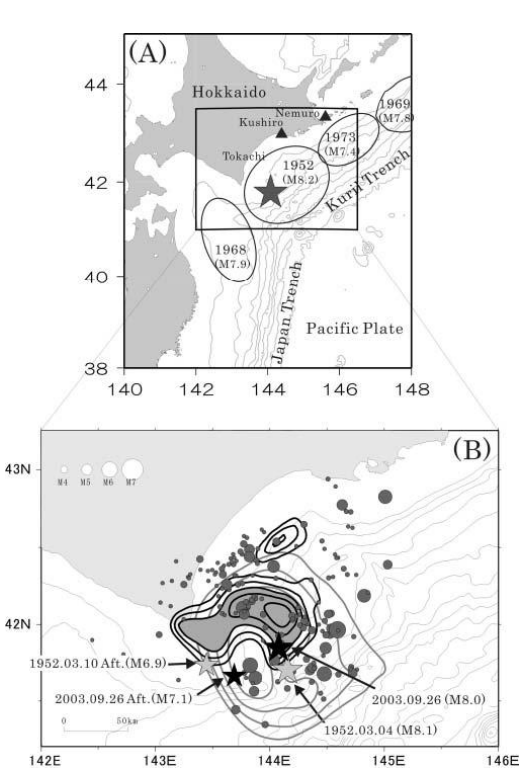

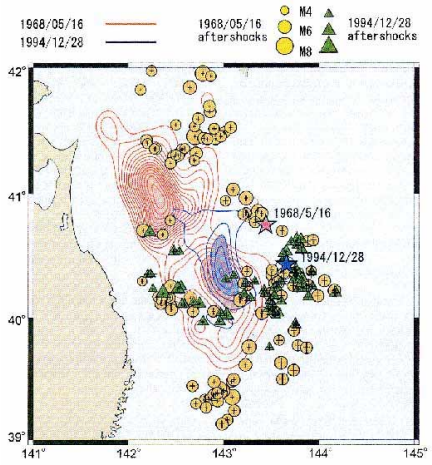

Fig. 13. Some proofs of the repetition of asperities. Left: Slip distributions for the 1952 and 2003 Tokachi-oki earthquakes (after Yamanaka and Kikuchi [28]). Right: Spatial distribution of the moment release and aftershocks for the 1968 Tokachi-oki and 1994 Sanriku-Haruka-oki earthquakes. (after Nagai *et al*. [30]).

CONCLUSIONS

We propose a recipe for predicting strong ground motions from future large earthquakes for inland crustal earthquakes caused by specific active faults and subduction-zone earthquakes. The recipe is made by the source characterization based on the multiple-asperity source model, and the hybrid method for simulating ground motions. The source model is characterized by three kinds of parameters, which we call: outer, inner, and extra fault parameters. The outer fault parameters define the entire source area for possible earthquake. The inner fault parameters are parameters characterizing fault heterogeneity inside the fault area. The extra fault parameters are related to the propagation pattern of the rupture.

The validity and applicability of the procedures for characterizing the earthquake sources for

strong ground prediction are examined in comparison with the observed records and broad-band simulated motions for the 1995 Kobe and the 2003 Tokachi-oki earthquakes. In future directions, strong ground motions taking into account the source dynamics are encouraged to constrain fault parameters.

ACKNOWLEDGEMENTS

We are grateful to Takao Kagawa and Ken Miyakoshi for their contributions at the early stage of this study. We used near-source ground motion data of KiK-net and CEORKA. GMT by Wessel and Smith [36] was used for making several figures. This work was supported in part by the Special Coordination Funds titled 'Study on the master model for strong ground motion prediction toward earthquake disaster mitigation' from the Ministry of Education, Science, Sports and Culture of Japan.

REFERENCES

1. Somerville P, Irikura K, Graves R, Sawada S, Wald D, Abrahamson N, Iwasaki Y, Kagawa T, Smith N, Kowada A. "Characterizing earthquake slip models for the prediction of strong ground motion." Seism. Res. Lett., 1998; 70: 59-80.
2. Miyake H, Iwata T, Irikura K. “Source characterization for broadband ground-motion simulation: Kinematic heterogeneous source model and strong motion generation area.” Bull. Seism. Soc. Am., 2003; 93: 2531-2545.
3. Das S, Kostrov BV. "Fracture of a single asperity on a finite fault." In Earthquake Source Mechanics, Geophysical Monograph 37, Maurice Ewing Series vol. 6, American Geophysical Union, 1986; 91-96.
4. Irikura K, Kamae K. "Strong ground motions during the 1948 Fukui earthquake." Zisin, 1999; 52: 129-150 (in Japanese).
5. Wald DJ, Helmberger DV, Hartzell SH. “Rupture model of the 1989 Loma Prieta earthquake from the inversion of strong-motion and broadband teleseismic data.” Bull. Seism. Soc. Am., 1990; 80: 1079-1098.
6. Mai PM, Beroza GC. “Source scaling properties from finite-fault-rupture models.” Bull. Seism. Soc. Am., 2000; 90: 604–615.
7. Boatwright J. "The seismic radiation from composite models of faulting." Bull. Seism. Soc. Am., 1988; 78: 489-508.
8. Madariaga R. “High-frequency radiation from crack (stress drop) models of earthquake faulting.” Geophys. J. R. Astron. Soc., 1977; 51: 625-651.
9. Madariaga, R. “On the relation between seismic moment and stress drop in the presence of stress and strength heterogeneity.” J. Geophys. Res., 1979; 84: 2243-2250.
10. Miyakoshi K. “Source characterization for heterogeneous source model.” Chikyu Monthly, 2002; extra 37: 42-47.
11. Irikura K, Miyake H. “Prediction of strong ground motions for scenario earthquakes.” Journal of Geography, 2001; 110: 849-875 (in Japanese with English abstract).
12. Wells DL, Coppersmith KL. "New empirical relationships among magnitude, rupture width, rupture area, and surface displacement." Bull. Seism. Soc. Am., 1994; 84: 974-1002.
13. Hanks TC, Bakun WH. “A bilinear source-scaling model for M–log A observations of continental earthquakes.” Bull. Seism. Soc. Am., 2002; 92: 1841–1846.
14. Scholz CH. “The mechanics of earthquakes and faulting.” Cambridge University Press, 2002.
15. Scholz CH. “Scaling laws for large earthquakes: Consequences for physical models.” Bull. Seism. Soc. Am., 1982; 72: 1-14.

16. Shaw BE, Scholz CH. “Slip-length scaling in large earthquakes: Observations an theory and implications for earthquake physics.” Geophys. Res. Lett., 2001; 28: 2995-2998.
17. Asano K. “Quantitative estimation of source rupture process and strong ground motion characteristics of the 2002 Denali, Alaska, earthquake.” Master Thesis for Kyoto University, 2004.
18. Eshelby JD. "The determination of the elastic field of an ellipsoidal inclusion, and related problems," Proc. Roy. Soc., 1957; A241: 376-396.
19. Satoh T. “Short-period spectral level of intraplate and interplate earthquakes occurring off Miyagi prefecture.” Journal of JAEE, 2004; 4, 1-4 (in Japanese with English abstract).
20. Morikawa N, Fujiwara H. “Source and path characteristics for off Tokachi-Nemuro earthquakes.” Programme and Abstracts for the Seismological Society of Japan, 2003 Fall Meeting, 2003; P104 (in Japanese).
21. Dan K, Watanabe T, Sato T, Ishii T. “Short-period source spectra inferred from variable-slip rupture models and modeling of earthquake fault for strong motion prediction.” Journal of Struct. Constr. Engng. AIJ, 2001; 545: 51-62.
22. Irikura K, Miyake H, Iwata T, Kamae K, Kawabe H, Dalguer LA. “Recipe for predicting strong ground motion from future large earthquake.” Anuuals of Disas. Prev. Res. Inst., Kyoto University, 2003; 46B: 105-120 (in Japanese with English abstract).
23. Nakata T, Shimazaki K, Suzuki Y, Tsukuda E. "Fault branching and directivity of rupture propagation." Journal of Geography, 1998; 107: 512-528 (in Japanese).
24. Kame N, Yamashita T. “Dynamic branching, arresting of rupture and the seismic wave radiation in self-chosen crack path modeling.” Geophys. J. Int., 2003; 155: 1042-1050.
25. Irikura K, Miyake H, Iwata T, Kamae K, Kawabe H. “Revised recipe for predicting strong ground motion and its validation.” Proceedings of the 11th Japan Earthquake Engineering Symposium, 2002; 567-572 (in Japanese with English abstract).
26. Kamae K, Irikura K. “Rupture process of the 1995 Hyogo-ken Nanbu earthquake and simulation of near-source ground motion.” Bull. Seism. Soc. Am., 1998; 88: 400-412.
27. Kamae K, Kawabe H. “Source model composed of asperities for the 2003 Tokachi-oki, Japan, earthquake (MJMA=8.0) estimated by the empirical Green's function method.” Earth Planets Space, 2003 (in press).
28. Yamanaka Y, Kikuchi M. “Source process of the recurrent Tokachi-oki earthquake on September 26, 2003,inferred from teleseismic body waves.” Earth Planets Space, 2003; 55: e21–e24.
29. Kikuchi M, Yamanaka Y. “Rupture processes of past large earthquakes = Identification of asperities.” Seismo, 2001; 5: 6-7.
30. Nagai R, Yamanaka Y, Kikuchi M. “Comparative study on the source processes of recurrent large earthquakes in Sanriku-oki region: The 1968 Tokachi-oki earthquake and the 1994 Sanriku-oki earthquake.” Zisin, 2001; 54: 267-280 (in Japanese with English abstract).
31. Wald DJ, Heaton TH. “Spatial and temporal distribution of slip for the 1992 Landers, California, earthquake.” Bull. Seism. Soc. Am., 1994; 84: 668-691.
32. Lee YH, Wu WY, Sugiyama Y, Azuma T, Kariya Y. “Displacements and segmentation of the surface fault, 1999 Chi-Chi, Taiwan, earthquake.” EOS Trans. Am. Geophys. Union, 1999; 81: 882.
33. Iwata T, Sekiguchi H, Pitarka A. "Source and site effects on strong ground motions in near-source area during the 1999 Chi-Chi, Taiwan, earthquake." EOS Trans. Am. Geophys. Union, 2000; 82: 882.
34. Wyss M, Schorlemmer D, Wiemer S. “Mapping asperities by minima of local recurrence time; San Jacinto-Elsinore fault zones.” J. Geophys. Res., 2000; 105: 7829-7844.
35. Nishigami K. “Deep crustal heterogeneity along and around the San Andreas fault system in central California and its relation to the segmentation.” J. Geophys. Res., 2000; 105; 7983-7998.
36. Wessel P, Smith WHF. "New version of the Generic Mapping Tools released." EOS Trans. Am. Geophys. Union., 1995; 76: 329.